APL Materials

Catalytic materials for efficient electrochemical production of hydrogen peroxide

Cite as: APL Mater. **8**, 050701 (2020); https://doi.org/10.1063/5.0002845
Submitted: 28 January 2020 . Accepted: 08 April 2020 . Published Online: 04 May 2020

Jaejung Song, and Seungho Cho

Catalytic materials for efficient electrochemical production of hydrogen peroxide

Cite as: APL Mater. 8, 050701 (2020); doi: 10.1063/5.0002845
Submitted: 28 January 2020 • Accepted: 8 April 2020 •
Published Online: 27 April 2020

Jaejung Song and Seungho Cho[a)]

AFFILIATIONS

School of Materials Science and Engineering, Ulsan National Institute of Science and Technology (UNIST), Ulsan 44919, South Korea

[a)]Author to whom correspondence should be addressed: scho@unist.ac.kr

ABSTRACT

Hydrogen peroxide (H_2O_2), the simplest peroxide consisting of only hydrogen and oxygen, is globally used as a green oxidant. It is also a promising fuel source, and it can be produced on large scales in centralized containers. H_2O_2 is mainly produced by the anthraquinone process, but it involves energy-consuming reactions and generates organic waste. As the demand for H_2O_2 continues to grow, alternative technologies that overcome these drawbacks are sought for its generation. The generation of H_2O_2 through the redox reaction of water and oxygen can be a low-cost, sustainable, and efficient production method. However, this reaction requires active and stable catalysts. In general, H_2O_2 can be generated by the oxidation of H_2O at the anode of an electrochemical cell. Alternatively, H_2O_2 can also be formed by the reduction of O_2 at the cathode. Despite the progress in the development and advancement of materials that catalyze these reactions, further research is required to increase the electron transport rates and active sites of the catalyst. In this article, we review the available catalytic materials for the electrochemical production of H_2O_2 and provide a summary and outlook of this field.

I. INTRODUCTION

Hydrogen peroxide (H_2O_2) was first artificially synthesized in 1818 by Baron Thenard, a French chemist.[1] H_2O_2 is recognized as one of the 100 most historically significant chemicals, and it is produced industrially on a very large scale.[2] It is used as a reagent in chemical,[3–6] pulp industries,[7,8] wastewater treatment,[9,10] and fuel cell technologies.[11] As it is completely soluble in water, which enables its easy transportation, it is regarded as an ideal energy carrier alternative to hydrogen (H_2) gas in the energy field. At present, H_2O_2 is predominantly produced by the anthraquinone process.[11] However, this process is not eco-friendly because it involves multistep reactions; it requires high energy input for the hydrogenation and further oxidation of alkylanthraquinone used as the precursor. In addition, alkylanthraquinone is not completely converted to anthraquinone because its chemical reactivity is moderate, which can lead to several undesired side reactions.[12] Furthermore, anthraquinone should be continuously replenished to maintain a satisfactory rate of H_2O_2 production. Therefore, there is a demand for the development of alternative H_2O_2 production methods, for both environmental and economic reasons.[11,13] Several articles have previously reviewed the established anthraquinone method and alternative methods of H_2O_2 production in detail.[7,11,14–17] This mini-review provides a brief overview of this field and focuses on the most recent research progress in the development of catalysts for H_2O_2 synthesis.

The alternative approaches for H_2O_2 production can be divided into three major categories: direct H_2O_2 synthesis,[7,14] photocatalyzed H_2O_2 synthesis,[16,18] and electroreduction of O_2 (Fig. 1).[17] Each of these methods has its advantages, and each has been developed gradually with the development of catalytic materials that boost the redox reactions of the H_2/O_2/water (H_2O) system. Among these approaches, the direct synthesis of H_2O_2 from H_2 and O_2 gases is efficient. Direct synthesis can be accomplished through noble metal catalysis,[19,20] the fuel cell method,[14,21] and plasma methods.[22] However, this approach requires precisely controlled amounts of H_2 and O_2 gases because the H_2/O_2 mixture can explode over a wide range of H_2 or O_2 concentrations, which makes it difficult to implement

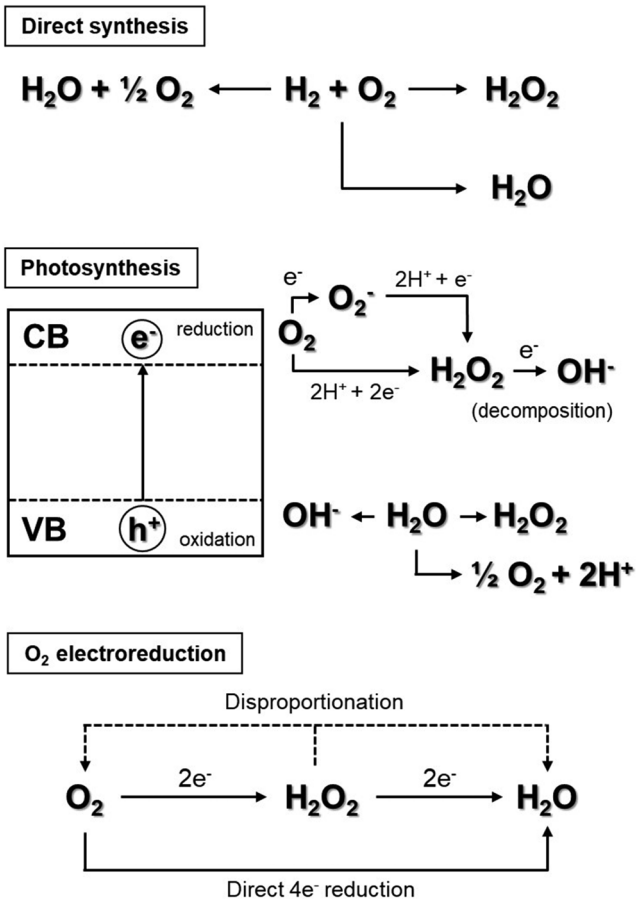

FIG. 1. Pathways for H_2O_2 production: direct synthesis, photocatalysis, and electroreduction of O_2.

it in industries. Some inert gases, such as nitrogen, carbon dioxide (CO_2), and argon, can, however, be included into the H_2/O_2 mixture to mitigate the risk of explosion.

In comparison, the use of photocatalytic systems for H_2O_2 production has many merits, and it has been continuously studied to better understand the associated advantages.[23] This approach is safer than the direct synthesis because H_2 gas is not used. Instead, abundantly available H_2O and O_2 are the only reagents required, and no toxic by-products are generated, which makes it a green method. The process starts from the photoexcitation of the catalyst to induce charge separation in its band structure. Light-induced electrons mediate the reduction of O_2 to H_2O_2, while the photoexcited holes oxidize H_2O to H_2O_2. Furthermore, H_2O_2 can also be generated by the two-electron oxidation of H_2O on catalytic anodes.[24–26] However, this method suffers from low H_2O_2 selectivity because electrons and holes can also induce the decomposition of H_2O_2.

Finally, the synthesis of H_2O_2 by the electrochemical reduction of O_2 is also a promising alternative. In this process, noble metals, metal alloys, and carbon-based materials are used as catalytic materials either individually or in combination.[27] These electrocatalysts have been developed to achieve high efficiency, selectivity, and even stable properties in the two-electron reduction process. Since the discovery of the Electro-Fenton (EF) reactions, O_2 reduction has been developed further, leading to improved H_2O_2 production.[28] H_2O_2 can be produced by the *in situ* reduction of the OH* radical on the surface of a catalyst-loaded cathode in a treated solution fed with O_2 or air.[29] However, as O_2 might be reduced via the direct four-electron or two-electron pathways, there is a need to develop efficient electrocatalysts with high selectivity for the reduction of O_2 to H_2O_2.

In general, H_2O_2 can be generated by electron- and proton-associated reactions of O_2 and H_2O, which can be categorized as follows: (i) direct synthesis from H_2 and O_2; (ii) $2e^-/2H^+$ oxidation of H_2O; (iii) $2e^-/2H^+$ reduction of O_2; and (iv) the combination of the $4e^-/4H^+$ oxidation of H_2O and the $2e^-/2H^+$ reduction of O_2. The electrochemical synthesis of H_2O_2 involves competitive H_2O_2 generation and decomposition reactions. The development of catalysts for H_2O_2 synthesis is not simple because catalysts generally promote both of these competing reactions. An ideal catalyst should promote the completion of redox reactions to H_2O_2 and also facilitate the rapid release of H_2O_2 from the reaction site before further

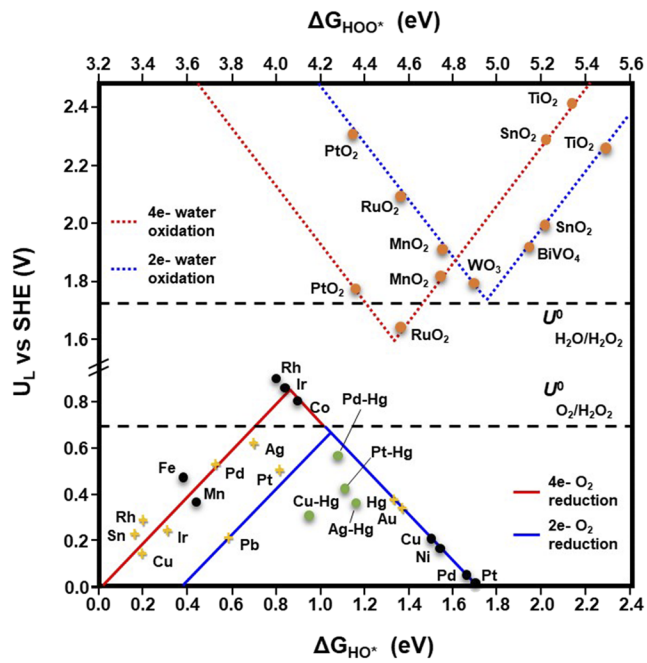

FIG. 2. Theoretical volcano plot for two-electron (blue) and four-electron (red) redox reactions of O_2 or H_2O, including the potentials for various materials under ambient conditions. The solid and dashed lines represent reduction and oxidation reactions, respectively. The catalysts are categorized as pure metal (yellow), metal alloy (green), metal:nitrogen/carbon (black), and metal oxide (orange) catalysts. The equilibrium potentials for the two-electron reduction of O_2 and the two-electron oxidation of H_2O are shown as dotted and dashed lines, respectively. U_L represents the theoretical limiting potential, and SHE represents the standard hydrogen electrode. Adapted with permission from Yang *et al.*, ACS Catal. **8**, 4064 (2018) and Viswanathan *et al.*, J. Phys. Chem. Lett. **6**, 4224 (2015). Copyright 2018 and 2015 American Chemical Society.

oxidation or reduction to H_2O or O_2, respectively. Therefore, many studies have focused on developing catalysts that show high selectivity in the oxidation of H_2O and the reduction of O_2 to H_2O_2. Figure 2 shows the calculated limiting potential (U_L) as a function of free energy change (ΔG) for the two- or four-electron reactions on various materials. Density functional theory (DFT) calculations aid the design and application of catalysts suitable for H_2O_2 synthesis. Such catalysts are mainly metals, carbon-based materials, and transition metal oxides, and these materials exhibit both small overpotentials and high H_2O_2 selectivities.[30–32] In addition, studies on the scale-up of the reaction for industrialization are also being actively pursued and reviewed.[11,14] This manuscript briefly and broadly surveys the catalytic materials used in H_2O_2 synthesis, and in particular, their modification for achieving efficient electrochemical H_2O_2 generation.

II. CATALYTIC MATERIALS FOR ELECTROCHEMICAL H_2O_2 GENERATION

Various materials can act as catalysts with high selectivity in H_2O_2 synthesis. Carbon-based materials have been widely developed and used because of their high performance, durability, and economic benefit. Meanwhile, metal, alloy, and their oxide forms also have superior catalytic abilities, and their syntheses and surface modification have been studied well. To achieve high efficiency, the electrode and catalytic materials can be developed as nanostructures. Smaller particles or structures provide a higher specific surface area and hence more active sites. In addition, small particles or pores induce high O_2 bubble binding affinity, which can enhance the H_2O_2 selectivity. For instance, decreasing the size of platinum nanoparticles increases the efficiency of the generation of H_2O_2 from O_2.[33] In the following subsections, we provide an account of the catalytic materials available for the efficient electrochemical production of H_2O_2.

A. Carbon-based materials

Carbon materials can be easily prepared and used in industrial applications that require chemical and mechanical stability.[34] Therefore, they have been widely studied, and their activities have been shown to be comparable to or even better than those of other H_2O_2 catalysts.[15,16,35] Hitherto, carbon materials, such as graphite,[36–39] graphene,[40,41] and carbon nanotubes (CNTs),[42,43] have been adopted in various forms, for example, as powders and thin films, to promote O_2-reduction and H_2O-oxidation reactions in order to produce H_2O_2. To further promote the catalytic activities and electron transfer rates, pores and/or sufficient defects can be deliberately introduced into these catalysts. However, a catalyst with high porosity can decrease the H_2O_2 output by impeding H_2O_2 release from the reaction sites.[44] Therefore, the degree of porosity and structural defects should be optimized precisely.

Graphite has been used as a basic carbon support to enhance the efficiency of H_2O_2 production. For example, Yang *et al.* fabricated a gas diffusion electrode (GDE), in which carbon black was deposited on graphite gas diffusion layers[45] to catalyze the production of H_2O_2 through O_2 reduction. Owing to the porous structure of the electrode, which has hydrophobic surfaces, the interfacial areas between the gas, electrolyte, and electrode were considerably higher, which is beneficial to the catalytic efficiency. Furthermore, Yu *et al.* deposited composites of carbon black and polytetrafluoroethylene (PTFE) emulsion on graphite to improve H_2O_2 production.[46] They optimized the performance of the catalyst layer in the GDE to achieve an accumulation of H_2O_2 of 1855 mg l^{-1} in 180 min at a flow rate of 0.05 (O_2) l min^{-1}. Furthermore, annealing of the graphite enhanced the H_2O_2 selectivity, owing to the enlargement of the hydrophobic areas where the diffusion of O_2 to the electrode could be accelerated. Perez *et al.* fabricated carbon cathodes with different PTFE loadings to determine the optimal permeability of the catalytic surface.[47] Upon the calcination of the electrode, the accumulation of H_2O_2 increased by more than one order of magnitude. They demonstrated that structural modification was responsible for the observed rapid reactions at the diffusion electrodes.

Furthermore, graphene, a single layer of graphite with a two-dimensional (2D) honeycomb-like structure, has also been applied in H_2O_2 production owing to its excellent optical, mechanical, electrical, thermal, and physicochemical properties, as well as a high specific surface area.[40,48] Yang *et al.* developed a hybrid electrode with carbon black and electrochemically exfoliated graphene.[48] The O_2-reduction reactions (ORRs) were promoted owing to higher rates of electron transfer in the exfoliated graphene electrode without a change in the mechanism of the ORR. Furthermore, the introduced graphene increased the number of active sites and the hydrophilicity of the cathode surface, thus leading to enhanced O_2 diffusion. The efficiency of the catalytic electrode in H_2O_2 production was found to be 7.7 mg cm^{-2} h^{-1}, with a relatively low energy consumption of 9.7 kW h kg^{-1}. Reduced graphene oxide (rGO), which has unique properties, can also be used as a co-catalyst and electron mediator. As its Fermi level can be adjusted, rGO can be used along with other semiconductors with a suitable band structure to serve as an electron transfer medium. Kim *et al.* synthesized highly selective and efficient rGO-based electrocatalysts through the mild thermal reduction of GO (mrGO) for generating H_2O_2 from O_2.[49] Through spectroscopic and *in situ* Raman spectroelectrochemical analyses, they confirmed that the sp^2-hybridized carbons near the ring ether defects along the mrGO sheet edges are the most active sites for peroxide production. Furthermore, they reported that the annealing of the catalyst further improved the electrocatalytic O_2 reduction. The derivatives of the mrGO electrocatalysts exhibited highly selective and stable activity in peroxide synthesis at low overpotentials under basic conditions, which was unprecedented when the study was reported.[49]

Carbon nanotubes (CNTs), which exhibit π–π stacking interactions, can be utilized in redox reactions because they can accept, transport, and store electrons.[50] They have been prepared in both pure and modified forms. Khataee *et al.* tested three carbon-based materials (bare graphite, activated carbon/graphite, and CNT/graphite) to increase the catalytic activity.[51] CNT/graphite was found to be the most efficient catalyst; the H_2O_2 productivity under the catalysis of this composite was nearly three or seven times higher than that of activated carbon/graphite or bare graphite, respectively. Zhang *et al.* fabricated a modified electrode using N-functionalized CNTs to enhance the H_2O_2 generation efficiency in the EF system.[52] This electrode provided a higher H_2O_2 formation rate than both graphite and bare CNT electrodes at a potential of −0.85 V. The concentrations of H_2O_2 produced by the graphite, CNT, and

N-functionalized CNT electrodes were 92.59 mg l^{-1}, 103.97 mg l^{-1}, and 145.62 mg l^{-1}, respectively. Furthermore, metal-decorated CNTs exhibit high electron transfer and generation rates owing to their modified bandgap structures and high reducing activities.[53] Recently, Jiang *et al.* synthesized M-CNTs (M: metal atom) and discovered that M–C–O is an efficient catalytic motif for H_2O_2 generation. It showed high selectivity (above 95%) in both alkaline and neutral conditions (Fig. 3).[54] Specifically, Fe–C–O was identified as a highly active and selective motif for reducing O_2 to H_2O_2. Through DFT calculations, considering all the possible sites of metal atom binding, the ORR activity and selectivity of different motifs were examined for a structure with a single Fe atom coordinated to a 2D carbon sheet, with and without O species. The calculations indicated that the C atoms of the Fe–C–O motifs could be selective for the two-electron-mediated production of H_2O_2, over the $4e^-$ product to H_2O.

Considering the progress made so far, there is significant room for improving the performance of catalysts for efficient H_2O_2 production. This could be achieved by modifying the carbon materials through strategies, such as metal nanoparticle loading, morphology tuning, or elemental doping. H_2O_2 production is known to depend on the surface area and band structure of the catalyst, which can be adjusted by controlling the ratio of the metal nanoparticles to the carbon structures. Figure 4 summarizes the catalytic performance of various types of catalysts in H_2O_2 production.[11] It is clear from Fig. 4 that the specific activity of Pt–Hg/C (metal on carbon) is 4–5 times higher than that of polycrystalline Pt–Hg (without carbon). The Pd–Au/C catalyst also showed higher selectivity and higher mass activity than those of the Pd–Au nanoparticles (NPs). Furthermore, Choi *et al.* reported that Pt NPs coated with amorphous carbon layers could induce single O atom adsorption of O_2 on their surface.[55]

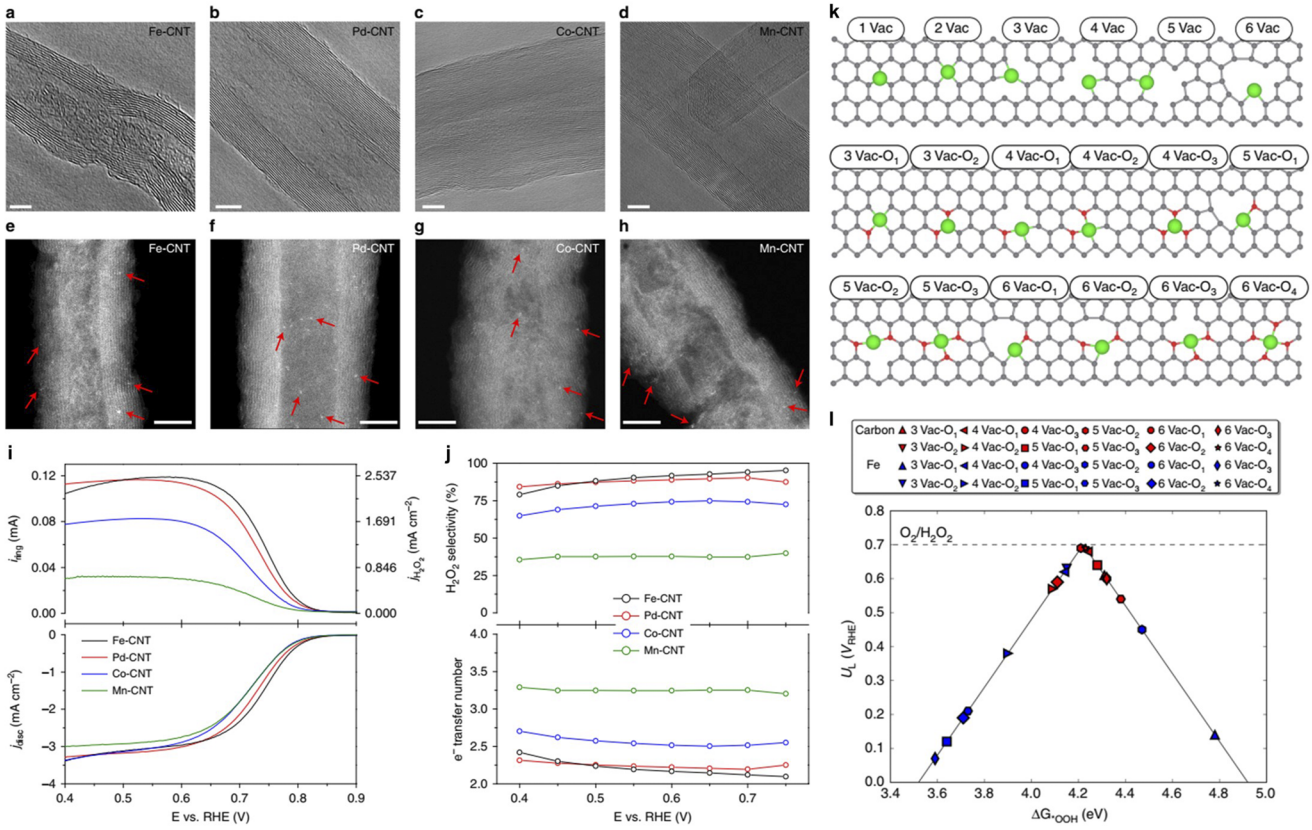

FIG. 3. Scanning transmission electron microscopy (STEM) images of [(a) and (e)] Fe-, [(b) and (f)] Pd-, [(c) and (g)] Co-, and [(d) and (h)] Mn-CNT. Bright dots in the high-angle annular dark-field STEM images (marked by red arrows) show single metal atoms. Scale bars are 5 nm. [(i) and (j)] ORR performances of M-CNT catalysts cast onto rotation ring disk electrodes in 0.1M KOH. (i) Linear sweep voltammetry of the CNT background and Fe-, Pd-, Co-, and Mn-CNT catalysts recorded at 1600 rpm and a scan rate of 5 mV s^{-1}, together with the detected H_2O_2 currents on the ring electrode (upper panel) at a fixed potential of 1.2 V vs reversible hydrogen electrode. (j) Calculated H_2O_2 selectivity and electron transfer number during the potential sweep. [(k) and (l)] DFT calculations of the ORR activity and selectivity on different motifs. (k) All configurations for a single Fe atom coordinated with C atoms, with and without O species. Green, red, and gray colors denote Fe, O (or N), and C atoms, respectively. (l) The calculated ORR activity volcano plot for two-electron-mediated pathway to H_2O_2. Red and blue symbols indicate *OOH adsorption at C and Fe, respectively. The equilibrium potential of O_2/H_2O_2 is shown as a black dashed line. Some of the points are not shown in the volcano plot as their binding energies are out of range. Reprinted with permission from Jiang *et al.*, Nat. Commun. **10**, 3997 (2019). Copyright 2019 Nature Publishing Group.

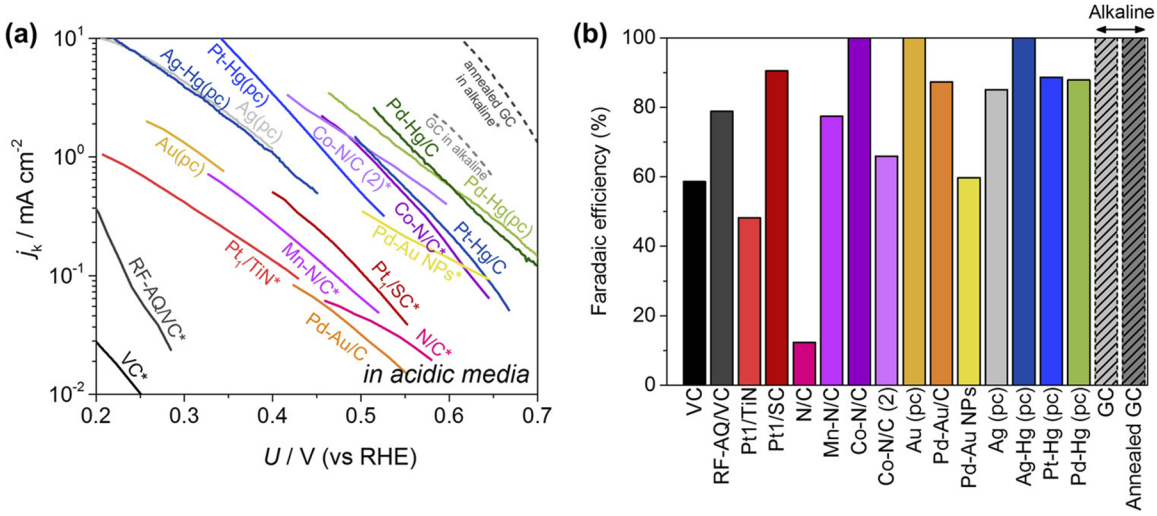

FIG. 4. Overview of different catalysts used in H_2O_2 production. (a) Mass-transport-corrected Tafel plots of kinetic current densities in acidic media based on rotating disk electrode or rotation ring disk electrode measurements. (b) Faradaic efficiency for each electrocatalyst. Reprinted with permission from Yang *et al.*, ACS Catal. **8**, 4064 (2018). Copyright 2018 American Chemical Society.

The tuning of the morphology of a catalyst not only allows us to increase the active sites, but also to modify the bandgap structure. Recently, Sa *et al.* fabricated an ordered graphitic mesoporous carbon (GOMC) material for H_2O_2 production via the ORR in 0.1M KOH.[32] They showed that additional oxidative treatment of the graphitic carbon could preferentially generate active oxygenated species at the carbon edge. The experimental data suggested that a faster heterogeneous electron transfer was responsible for the higher ORR activity of the oxidized and edge-rich carbon catalysts. GOMC could stably catalyze the production of H_2O_2 for 16 h with the Faradaic efficiency reaching 99%, and the accumulated H_2O_2 concentration was 24 mM.

It has been shown that doped carbon materials can have significant catalytic effects when additional elements are introduced into carbon frameworks, and this aspect has been actively studied recently. Various elements including boron (B),[27] nitrogen (N),[56] phosphorus (P),[57] sulfur (S),[58] and transition metals[30] have been investigated as dopants of carbon materials. Chen *et al.* designed B–carbon–N (BCN) materials by varying the ratio of B and N precursors to increase the $2e^-$ ORR selectivity.[27] They demonstrated that the BN domains embedded in the co-doped graphitic structures facilitated higher activity and selectivity in the $2e^-$ ORR to H_2O_2 than the corresponding singly doped materials (B-doped or N-doped carbon). However, in some cases, the H_2O_2 selectivity of doped carbon materials was found to decrease owing to the increase in the electron transfer rates of dopants.[59] Therefore, it is not easy to determine the exact redox mechanisms, potentials, and reactivity according to the identities of the dopants. However, in general, dopants partially reorganize the localized electronic density on carbon lattices and generate polar regions; therefore, their influence on the electron transfer rate of carbon materials is not significant.[60,61] Recently, Jung *et al.* incorporated a Co–N_4 moiety in nitrogen-doped graphene for electrochemical H_2O_2 production.[30] This catalyst showed a high H_2O_2 productivity of 418 ± 19 mmol g_{cat}^{-1} h^{-1} at a catalyst loading of ~1 mg cm^{-2}. The fine-tuning of the interaction between a given metal atom and the surrounding atomic configuration of a catalyst is required for achieving high catalytic activity in H_2O_2 production. The changes in the activity of a catalyst upon doping thus originate mainly from the chemical effects of dopants.

In summary, carbon materials are excellent catalysts for H_2O_2 synthesis. However, they are relatively unstable in the presence of H_2O_2 in comparison with other catalysts, such as metals and metal oxides.[59] As the catalytic stability is indispensable for practical application, further studies are required to enhance the catalytic stabilities of carbon-based materials in H_2O_2 synthesis.

B. Pure metals and alloys

For efficient H_2O_2 generation, it is very important to investigate and calculate the associated enthalpy changes as well as activation energies, for both forward and reverse reactions of H_2O and O_2.[62] On this basis, noble metals, such as palladium, platinum, silver, and gold, have been applied in various ways to promote the 2-electron pathway of H_2O_2 synthesis. Among the noble metals, Pd is preferred as an electrochemical catalyst because of its activity in the ORR and O_2 evolution reaction.[63] Kim *et al.* investigated the changes in the activity of Pd catalysts in H_2O_2 synthesis according to the exposed crystal plane and particle size. They found that a larger particle size and the (111) crystal plane are favorable for this reaction.[64] Iwamoto *et al.* also reported that saturated active sites located on the (111) crystal plane of Pd particles are beneficial for the generation of H_2O_2 through a DFT study. They also determined that unsaturated active sites located at the crystal angles and crystal edges of Pd particles easily lead to the formation of H_2O as a by-product.[65] Au has been considered a potentially reactive metal among

precious metals for H_2O_2 formation for some time, based on theoretical calculations that predicted the stable formation of H_2O_2 molecules on its surfaces.[66] Such characteristics of Au have been practically demonstrated by various groups.[67] Furthermore, with respect to the catalyst size, small Au nanoclusters (~2 nm) have been shown to have active sites suitable for the synthesis of H_2O_2.[68,69] The rate of H_2O_2 formation was found to decrease with the increasing size of the Au nanoparticles. This tendency has also been experimentally proven with an Au/silica (SiO_2) catalyst; a catalyst consisting of Au nanoparticles with a mean diameter of 30 nm could produce H_2O but not H_2O_2. Therefore, when using materials based on precious metals as catalysts, it is important to consider the choice of element and their structure. According to DFT calculations, for catalysts based on a single metal, different reaction processes are possible in H_2O generation, depending on the element. In the cases of Pd, Pt, and Au catalysts, the dissociation of O_2 and OOH^* intermediate species, and the decomposition of H_2O_2 induce H_2O production.[70] Although pure precious metals have the potential to enable efficient H_2O_2 generation, noble metals are expensive, and they do not exhibit high H_2O_2 selectivity (~100%). Therefore, researchers have investigated metal alloys and composites as catalysts for practical application.

Bimetallic alloys have been studied as catalysts for achieving high catalytic performances in H_2O_2 synthesis. By alloying active metals and relatively inert metals, activation potentials can be enhanced by discrete reactive sites embedded in a relatively inert material (Fig. 2).[71] As Pd alloys exhibit better performance than pure metals,[72] the activities of Pd-,[73,74] Au-,[75] and Ru-based bimetallic catalysts[76] in H_2O_2 synthesis have been studied. Among them, Pd–Au has attracted significant attention,[77,78] while only a few studies on the Pd–Pt,[79] Ru–Pd,[76] or Pt–CuS_x[80] systems have been reported. Various Pd-based bimetallic nanoparticles have been shown to perform better than single metal catalysts.[81] Interestingly, metal alloy catalysts have exhibited enhanced H atom selectivity toward H_2O_2 compared to pure Pd catalysts. Studies on Pd-based catalysts have been reviewed previously.[81–83]

Typically, for H_2O_2 generation, two electrons should be transferred from a catalyst to O_2. The attachment of O_2 to Au is too weak for efficient electron transfer. However, O_2 binds strongly to Pd; therefore, the O–O bond can be cleaved easily, which is not beneficial for H_2O_2 generation (Fig. 5). Thus, alloying with Au can lead to appropriate O_2–metal binding strength for two-electron transfer, resulting in high H_2O_2 generation efficiency.[84] Pritchard *et al.* synthesized both a homogeneous Pd–Au alloy and core–shell Pd–Au particles.[85] The homogeneous alloy nanoparticles were prepared by the simultaneous addition and reduction of metal salts, whereas the core–shell structure was formed by the reduction of Pd followed by the reduction of Au (Fig. 6). They claimed that the incorporation of a small amount of Au into the Pd lattice affected the electronic structure of Pd, which could lead to significant enhancement in catalytic activity in H_2O_2 generation. Although high H_2O_2 production was observed for Au/Pd at a 1:2M ratio, side hydrogenation reactions of H_2O_2 were also promoted [Fig. 6(g)]. Edwards *et al.* demonstrated that nanocomposites with 2.5 wt. % Au–2.5 wt. % Pd exhibited significantly enhanced activity in H_2O_2 synthesis. Furthermore, the rate of H_2O_2 production under their catalysis was much higher than that under pure Pd and pure Au catalysts.[86] Moreover, the authors claimed that the Pd^0/Pd^{2+} ratio may also be an important factor in controlling a series of reduction and re-oxidation.[87]

Xu *et al.* observed that Pd catalysts alloyed with Pt could show improved activity in H_2O_2 synthesis.[79] The $Pd_{16}Pt_1$ alloy achieved a H_2O_2 production rate of 1.77 mol h^{-1} $g_{Pd}{}^{-1}$ and selectivity of 60%, while pure Pd showed a rate of 0.99 mol h^{-1} $g_{Pd}{}^{-1}$ and selectivity of 12%. However, the Pd–Pt alloys showed enrichment of Pt on their surfaces. The authors claimed that tuning the electronic structure of Pd with a small amount of Pt might help stabilize O_2 molecules on the Pd sites. After their formation from adsorbed

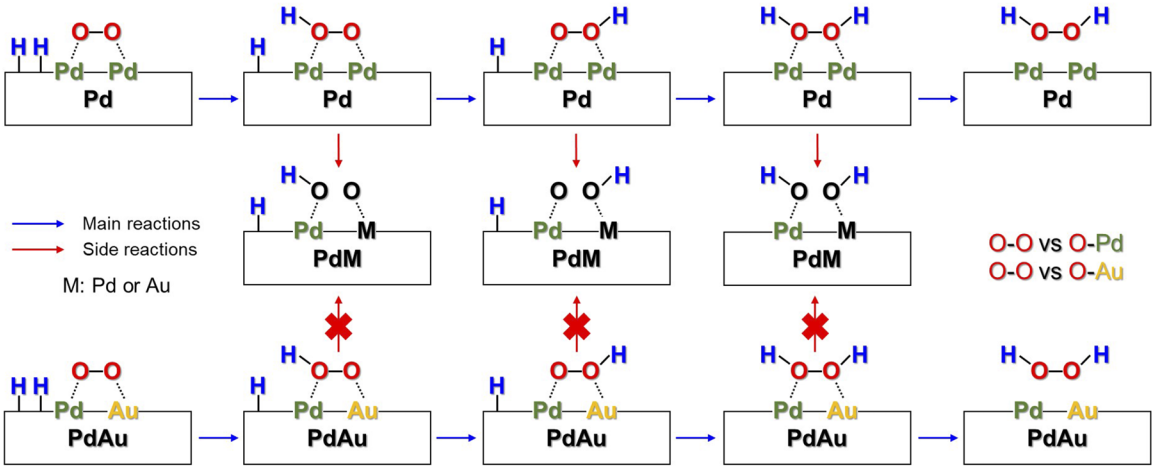

FIG. 5. Effect of the presence or absence of gold metal in O_2 and H_2O_2 chemisorption leading to hydrogen peroxide or water formation selectivity, respectively. The high activity of Pd and the high selectivity of Au play roles in the enhancement of H_2O_2 synthesis. This scheme is Reproduced with permission from J. Li and K. Yoshizawa, Catal. Today **248**, 142 (2015) and Pengfei *et al.*, Chin. J. Catal. **34**, 1002 (2013).[107] Copyright 2015 and 2013 Elsevier B.V.

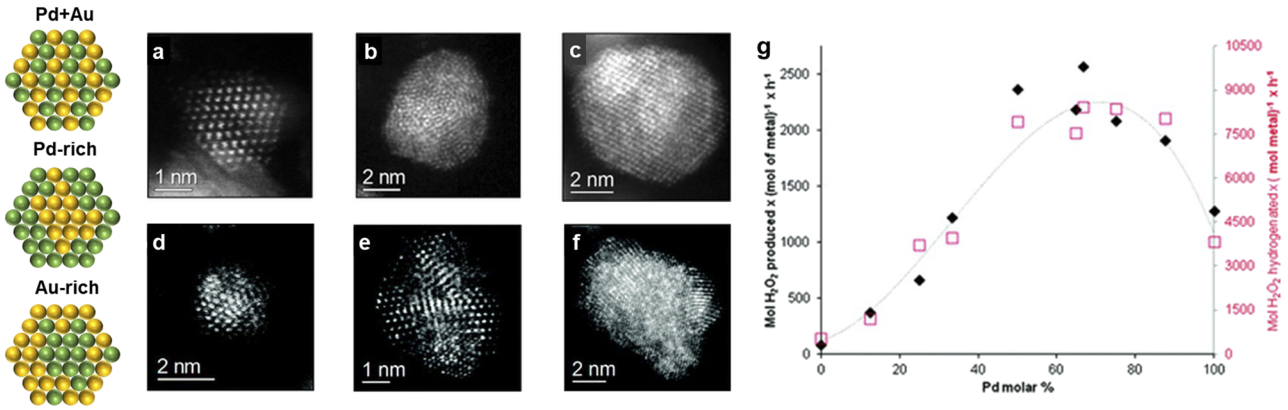

FIG. 6. Hydrogen peroxide synthesis using Pd–Au catalysts prepared by sol-immobilization with varying Pd and Au compositions. Transmission electron microscopy images of [(a)–(c)] homogeneous random alloys and [(d)–(f)] heterogeneous alloys of Pd and Au. The particles progressively become more Pd-rich and less Au-rich from (d) to (f). The smaller particles were Au-rich, whereas the larger ones tended to be Pd-rich. (g) Comparison of the specific activity of 1 wt. % Au–Pd/C with a Pd/Au molar ratio of 1.85 prepared by sol-immobilization in H_2O_2 synthesis and H_2O_2 hydrogenation. The H_2O_2 productivity was calculated after 30 min (solid black rhombuses), and the rates of H_2O_2 hydrogenation were calculated after 30 min (open red squares). Adapted with permission from Pritchard *et al.*, Langmuir **26**, 16568 (2010). Copyright 2010 American Chemical Society.

O_2, the OOH* radicals can produce H_2O_2. Thus, excess Pt on the shell layer deteriorated the catalytic performance by destabilizing the OOH* radicals.

When combining different kinds of metals for H_2O_2 synthesis, multiple characteristics of the resultant alloys and composites should be considered simultaneously. For example, as mentioned earlier, the loading of Au into Pd can enhance the H_2O_2 selectivity of Pd; however, the loading of Au can decrease the overall catalytic activity of the Pd–Au alloy. Some combinations of metals can have a high catalytic activity but poor performance retention. Therefore, a deeper understanding of the catalytic mechanisms of these metallic materials is required to meet the industrial demands of catalytic activity, selectivity, stability, and durability.

Noble metals are currently considered as one of the most efficient catalysts to generate H_2O_2. However, the high cost and scarcity of noble metals greatly hinder their large-scale application. Thus, to enable the industrial application of the catalysts for electrochemical production of H_2O_2, low-cost, earth-abundant, and highly stable electrocatalysts are required. Therefore, it is necessary to develop noble metal catalysts with high H_2O_2 catalytic efficiency with very low noble metal content.

C. Metal oxides

Metal oxides have been used in various applications owing to their earth-abundance, low cost of production, and chemical inertness. Metal oxides can also be used as catalysts for electrochemical or photocatalyzed generation of H_2O_2. Iridium or ruthenium oxides can induce anodic reactions at the lowest overpotentials,[88] but they tend to favor O_2 formation and are expensive for large-scale application.[89] Thus, less expensive metal oxides, such as titanium dioxide (TiO_2),[24,90] manganese oxide (MnO_x),[25] bismuth vanadate ($BiVO_4$),[26] and tin dioxide (SnO_2), have been actively investigated for H_2O_2 generation.[91] Some metal oxides have been studied as photocatalysts as well as electrocatalysts.[92] Electrons (e^-) and holes

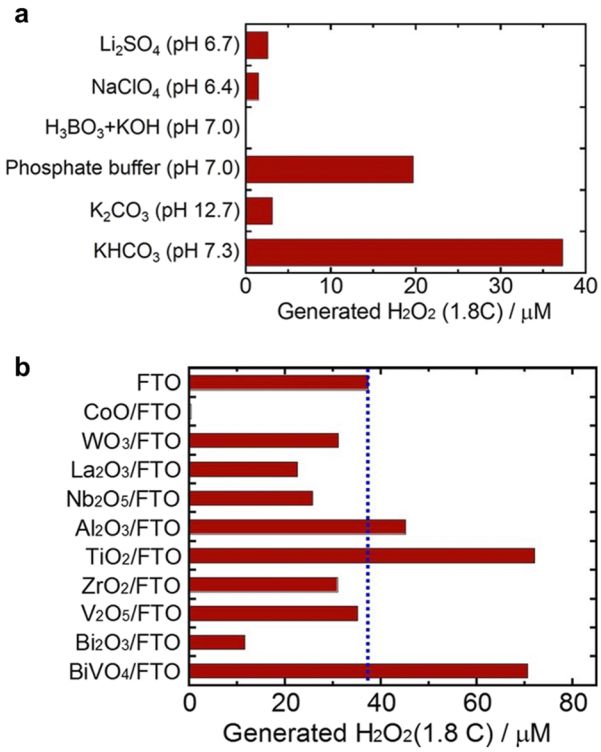

FIG. 7. (a) Oxidative H_2O_2 generation on a bare FTO electrode at the applied electric charge of 1.8 C at 0 V under CO_2 or Ar gas bubbling into various 0.5M aqueous solutions (35 ml) maintained in an ice bath (below 5 °C). (b) Comparison of H_2O_2 generation using anodes with various metal oxides loaded on FTO electrodes in an ice bath (below 5 °C) in a 0.5M $KHCO_3$ aqueous solution (35 ml) under CO_2 gas bubbling at an electric charge of 1.8 C and applied voltage of 3.0 V. Reprinted with permission from Fuku *et al.*, ChemistrySelect **1**, 5721 (2016). Copyright 2016 Wiley-VCH.

(h^+) generated through photocatalysis or electrocatalysis cause O_2 reduction and H_2O oxidation, respectively, in H_2O_2 redox reactions.[93] Fuku *et al.* tested the electrocatalytic activities of a fluorine-doped SnO_2 (FTO) substrate and FTO with various metal oxides in salt solutions for H_2O_2 production.[94] On bare FTO, H_2O_2 can be generated as expected from Fig. 2, and the H_2O_2-production efficiency increased significantly in the cases of an aqueous potassium bicarbonate ($KHCO_3$) electrolyte and a phosphate buffer [Fig. 7(a)]. Furthermore, this group applied various metal oxides on the FTO substrate to compare their electrocatalytic activities in H_2O_2 synthesis in a $KHCO_3$ aqueous solution. The data were consistent with the results of thermodynamic analysis, which suggested that WO_3, SnO_2, $BiVO_4$, and TiO_2 can catalyze the production of H_2O_2 (Fig. 2). The enhanced activities of FTO substrates supported by Al_2O_3, TiO_2, and $BiVO_4$ may be attributed to the favorable adsorption of HCO_3^- on acidic oxide surfaces [Fig. 7(b)].

TiO_2 has been widely studied as a catalyst for various reactions because of its high stability, biocompatibility, and useful physical, optical, and electrical properties.[95] The potential of the lowest unoccupied molecular orbital (LUMO) of TiO_2 (−0.19 V vs normal hydrogen electrode, pH 0) is lower than the potential for the two-electron reduction of O_2 (0.68 V). Therefore, the excited electrons of TiO_2 can promote the ORR for H_2O_2 generation. In addition, TiO_2 can be used as an anode material for the oxidation of H_2O. However, TiO_2 can hardly facilitate electron and hole transfers because of its relatively large bandgap; therefore, its onset potential is high for H_2O_2 generation. Furthermore, after the H_2O_2 binds to the surface of TiO_2, the intermediates (Ti–OOH complexes) can decompose to

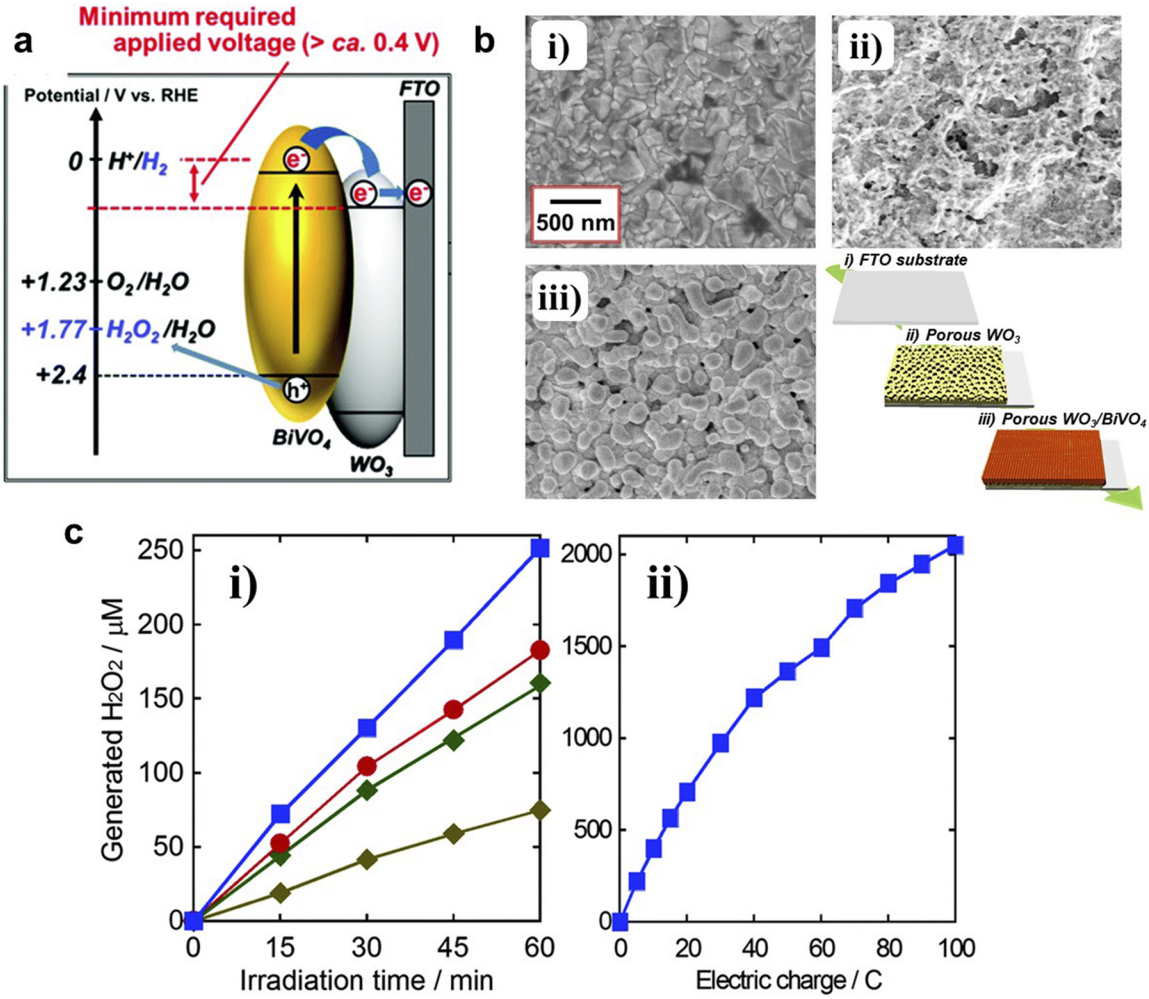

FIG. 8. (a) Energy diagram of the electrode system for the production and recovery of H_2O_2 and H_2 using a $WO_3/BiVO_4$ electrode. (b) Scanning electron microscopy images of (i) FTO, (ii) FTO with WO_3 underlayer, and (iii) FTO with WO_3 underlayer and $WO_3/BiVO_4$. (c) (i) Time courses of oxidative H_2O_2 generation in 0.1M (yellow rhombuses), 0.5M (green rhombuses), 1.0M (red circles), and 2.0M (blue squares) $KHCO_3$ electrolyte (35 ml) and (ii) oxidative H_2O_2 generation in a 2.0M $KHCO_3$ electrolyte under CO_2 gas bubbling in an ice bath (below 5 °C) at an applied voltage of 1.5 V, using a $WO_3/BiVO_4$ electrode. Reproduced with permission from K. Fuku and K. Sayama, Chem. Commun. **52**, 5406 (2016). Copyright 2016 The Royal Society of Chemistry.

Ti–OH and OH* radicals through reduction because TiO_2 has a high OH*-free energy.

$BiVO_4$ has a bandgap of 2.4 eV and is commonly used as a visible-light photosensitizer or electrocatalyst.[96] Specifically, it has been intensively investigated for splitting H_2O.[97] As the LUMO level of $BiVO_4$ is more negative compared with the two-electron O_2-reduction potential, it is also active in H_2O_2 production. $BiVO_4$ can also be used as a constituent of composites. Fuku *et al.* used a tungsten trioxide (WO_3)/$BiVO_4$ composite as a photoelectrocatalyst on a FTO anode for oxidative H_2O_2 production from H_2O along with the simultaneous production of H_2 gas on a Pt cathode (Fig. 8).[26] The WO_3/$BiVO_4$ oxide layer on FTO was confirmed through scanning electron microscopy, and the bicarbonate (HCO_3^-) electrolyte was found to permit stable oxidative H_2O_2 production and accumulation on the $BiVO_4$ surface, even at a lower voltage than the theoretical electrolysis voltage. Furthermore, the suppression of oxidative degradation could be accomplished by increasing the HCO_3^- concentration significantly at a low temperature. In addition, the same group also reported the oxidative and reductive H_2O_2 production from H_2O and O_2, respectively, by using a $BiVO_4$ anode and Au cathode without external bias.[98] By introducing the Au cathode, the two-electron reduction of O_2 was selectively catalyzed. In their follow-up study, to enhance the generation of H_2O_2, a mesoporous and amorphous aluminum oxide (Al_2O_3) layer was applied as an additional layer to inhibit the oxidative degradation of the generated H_2O_2 into O_2 on the electrode. The modified electrode provided high H_2O_2 selectivity (~80%) and catalytic stability.[99] Other metal oxide-coated electrodes were also tested for H_2O_2 generation. Their selectivity can be ranked as follows: Al_2O_3 > (zirconium dioxide) ZrO_2 > TiO_2 > SiO_2 ≫ cobalt oxide (CoO_x). The authors attributed the excellent selectivity on the WO_3/$BiVO_4$/Al_2O_3 photoanode to the blocking effect of the mesoporous Al_2O_3 layer, which inhibits oxidative H_2O_2 degradation into O_2 on the $BiVO_4$. They also reported an enhancement effect resulting from the increased HCO_3^- concentration around the electrode owing to the adsorption of HCO_3^- (a weak base) to the weakly acidic surface of Al_2O_3. Recently, the surface reactivity of the $BiVO_4$ anode has been investigated through a combination of experimental and computational studies.[100] The authors claimed that the adsorption of anion species can be promoted to inhibit H_2O_2 dissociation on the high index (−121) surface of the catalyst, compared with that on the low index (010) surface.

Various other oxides, such as WO_3,[101] Co_xO_y,[102] cerium oxide (CeO_2),[103] niobium pentoxide (Nb_2O_5),[104] tantalum pentoxide (Ta_2O_5),[105] and vanadium oxide (V_xO_y),[106] have also been used as anodic electrode materials to provide electrons. They can be used along with carbon-based materials in the form of nanoparticles to greatly increase their O_2-reduction activities. Carneiro *et al.* fabricated Nb_2O_5-based nanocomposites decorated with rGO to generate H_2O_2. The Nb_2O_5-rGO electrode provided a higher H_2O_2 output than the bare rGO electrode in both acidic and alkali conditions.[104] Ta_2O_5 nanoparticles mixed with carbon black were also investigated as catalytic materials for H_2O_2 synthesis.[105] Ta_2O_5 mixed with rGO exhibited a higher H_2O_2 output and selectivity than those of pure metal oxide or rGO. Metal oxides can also have activities for $4e^-$ O_2 reduction to H_2O. Therefore, synthesis methods and surface modification should be further developed to tune the physical or chemical properties for suppressing $4e^-$ O_2 reduction on metal oxides to achieve higher selectivities in H_2O_2 synthesis.

Metal oxides are considered as highly promising materials for the efficient catalysis of H_2O_2 generation from two-electron-mediated reactions. Compared with other materials, however, the number of reports on metal oxides as catalysts for H_2O_2 production is relatively small. Therefore, further studies should be conducted for enhancing the H_2O_2 catalytic activities of metal oxides because they are readily available and also incur low cost.

III. CONCLUSION AND OUTLOOK

This article outlined the catalytic materials that have been studied in the electrochemical generation of H_2O_2. Recent studies on carbon-based materials, metals, metal oxides, and their composites have shown that they have promising catalytic activities to enable the replacement of the anthraquinone process with other H_2O_2 synthesis routes. However, further challenges should be overcome before they can be applied in large-scale H_2O_2 production. The chemical decomposition of the as-generated H_2O_2 on the catalyst inhibits their practical application. Therefore, rational theoretical calculations and experiments should be conducted for the design of H_2O_2 catalysts. Such studies can assist the design of better catalysts to minimize overpotentials in order to produce H_2O_2 through the $2e^-$ oxygen reduction for high stability. The smart tailoring of materials for the optimal conversion of H_2O or O_2 to H_2O_2 through methods, such as size reduction, surface modification, doping, deliberate generation of defects, and heterostructuring, can lead to further improvement in electrochemical H_2O_2 generation. Therefore, active research is required to address the issues of catalytic instability and material costs toward overall process optimization and scale-up of the reaction.

ACKNOWLEDGMENTS

We acknowledge the 2020 Research Fund (Grant No. 1.200036.01) of UNIST (Ulsan National Institute of Science & Technology) for financial support. This work was also supported by the National Research Foundation of Korea (NRF) through a grant funded by the Korean government (MSIP; Ministry of Science, ICT & Future Planning; Grant Nos. NRF-2018R1C1B6002342 and NRF-2019M1A2A2065612).

REFERENCES

[1] L. J. Thénard, Ann. Chim. Phys. **8**, 306 (1818).
[2] K. Sato, M. Aoki, and R. Noyori, Science **281**, 1646 (1998).
[3] P. T. Tanev, M. Chibwe, and T. J. Pinnavaia, Nature **368**, 321 (1994).
[4] R. Noyori, M. Aoki, and K. Sato, Chem. Commun. **39**, 1977 (2003).
[5] B. S. Lane and K. Burgess, Chem. Rev. **103**, 2457 (2003).
[6] W. Zhan, L. Ji, Z.-M. Ge, X. Wang, and R.-T. Li, Tetrahedron **74**, 1527 (2018).
[7] J. M. Campos-Martin, G. Blanco-Brieva, and J. L. Fierro, Angew. Chem., Int. Ed. **45**, 6962 (2006).
[8] X.-S. Chai, Q. Hou, Q. Luo, and J. Zhu, Anal. Chim. Acta **507**, 281 (2004).
[9] K. Kosaka, H. Yamada, K. Shishida, S. Echigo, R. A. Minear, H. Tsuno, and S. Matsui, Water Res. **35**, 3587 (2001).
[10] M. Ksibi, Chem. Eng. J. **119**, 161 (2006).

[11] S. Yang, A. Verdaguer-Casadevall, L. Arnarson, L. Silvioli, V. Čolić, R. Frydendal, J. Rossmeisl, I. Chorkendorff, and I. E. Stephens, ACS Catal. **8**, 4064 (2018).
[12] R. Kosydar, A. Drelinkiewicz, and J. Ganhy, Catal. Lett. **139**, 105 (2010).
[13] S. Fukuzumi, Y. M. Lee, and W. Nam, Chem. - Eur. J. **24**, 5016 (2018).
[14] Y. Yi, L. Wang, G. Li, and H. Guo, Catal. Sci. Technol. **6**, 1593 (2016).
[15] Y. Jiang, P. Ni, C. Chen, Y. Lu, P. Yang, B. Kong, A. Fisher, and X. Wang, Adv. Energy Mater. **8**, 1801909 (2018).
[16] A. Torres-Pinto, M. J. Sampaio, C. G. Silva, J. L. Faria, and A. M. T. Silva, Catalysts **9**, 990 (2019).
[17] S. Siahrostami, A. Verdaguer-Casadevall, M. Karamad, D. Deiana, P. Malacrida, B. Wickman, M. Escudero-Escribano, E. A. Paoli, R. Frydendal, and T. W. Hansen, Nat. Mater. **12**, 1137 (2013).
[18] F. Shiraishi, T. Nakasako, and Z. Hua, J. Phys. Chem. A **107**, 11072 (2003).
[19] S. J. Freakley, Q. He, J. H. Harrhy, L. Lu, D. A. Crole, D. J. Morgan, E. N. Ntainjua, J. K. Edwards, A. F. Carley, and A. Y. Borisevich, Science **351**, 965 (2016).
[20] J. H. Lunsford, J. Catal. **216**, 455 (2003).
[21] I. Yamanaka, T. Onizawa, S. Takenaka, and K. Otsuka, Angew. Chem., Int. Ed. **42**, 3653 (2003).
[22] B. R. Locke and K.-Y. Shih, Plasma Sources Sci. Technol. **20**, 034006 (2011).
[23] Z. Haider, H.-I. Cho, G.-H. Moon, and H.-I. Kim, Catal. Today **335**, 55 (2019).
[24] J. Zhang and Y. Nosaka, J. Phys. Chem. C **117**, 1383 (2013).
[25] A. Izgorodin, E. Izgorodina, and D. R. MacFarlane, Energy Environ. Sci. **5**, 9496 (2012).
[26] K. Fuku and K. Sayama, Chem. Commun. **52**, 5406 (2016).
[27] S. Chen, Z. Chen, S. Siahrostami, D. Higgins, D. Nordlund, D. Sokaras, T. R. Kim, Y. Liu, X. Yan, and E. Nilsson, J. Am. Chem. Soc. **140**, 7851 (2018).
[28] E. Brillas, E. Mur, and J. Casado, J. Electrochem. Soc. **143**, L49 (1996).
[29] I. Sirés, E. Brillas, M. A. Oturan, M. A. Rodrigo, and M. Panizza, Environ. Sci. Pollut. Res. **21**, 8336 (2014).
[30] E. Jung, H. Shin, B.-H. Lee, V. Efremov, S. Lee, H. S. Lee, J. Kim, W. H. Antink, S. Park, and K.-S. Lee, Nat. Mater. **19**, 436 (2020).
[31] Z. Zheng, Y. H. Ng, D.-W. Wang, and R. Amal, Adv. Mater. **28**, 9949 (2016).
[32] Y. J. Sa, J. H. Kim, and S. H. Joo, Angew. Chem., Int. Ed. **58**, 1100 (2019).
[33] A. von Weber, E. T. Baxter, H. S. White, and S. L. Anderson, J. Phys. Chem. C **119**, 11160 (2015).
[34] Q. Xin, H. Shah, A. Nawaz, W. Xie, M. Z. Akram, A. Batool, L. Tian, S. U. Jan, R. Boddula, and B. Guo, Adv. Mater. **31**, 1804838 (2018).
[35] Z. Chen, S. Chen, S. Siahrostami, P. Chakthranont, C. Hahn, D. Nordlund, S. Dimosthenis, J. K. Nørskov, Z. Bao, and T. F. Jaramillo, React. Chem. Eng. **2**, 239 (2017).
[36] M. Assumpção, R. De Souza, D. Rascio, J. Silva, M. Calegaro, I. Gaubeur, T. Paixão, P. Hammer, M. Lanza, and M. C. Santos, Carbon **49**, 2842 (2011).
[37] F. Yu, M. Zhou, and X. Yu, Electrochim. Acta **163**, 182 (2015).
[38] Y. Wang, Y. Liu, K. Wang, S. Song, P. Tsiakaras, and H. Liu, Appl. Catal., B **165**, 360 (2015).
[39] J. Miao, H. Zhu, Y. Tang, Y. Chen, and P. Wan, Chem. Eng. J. **250**, 312 (2014).
[40] T. X. H. Le, M. Bechelany, S. Lacour, N. Oturan, M. A. Oturan, and M. Cretin, Carbon **94**, 1003 (2015).
[41] J. García-Serna, T. Moreno, P. Biasi, M. J. Cocero, J.-P. Mikkola, and T. O. Salmi, Green Chem. **16**, 2320 (2014).
[42] K. Gong, F. Du, Z. Xia, M. Durstock, and L. Dai, Science **323**, 760 (2009).
[43] R. Babaei-Sati and J. Basiri Parsa, New J. Chem. **41**, 5995 (2017).
[44] J. Park, Y. Nabae, T. Hayakawa, and M.-A. Kakimoto, ACS Catal. **4**, 3749 (2014).
[45] Y. Xu, L. Cao, W. Sun, and J. Yang, Chem. Eng. J. **310**, 170 (2017).
[46] X. Yu, M. Zhou, G. Ren, and L. Ma, Chem. Eng. J. **263**, 92 (2015).
[47] J. F. Pérez, C. Sáez, J. Llanos, P. Cañizares, C. López, and M. A. Rodrigo, Ind. Eng. Chem. Res. **56**, 12588 (2017).
[48] W. Yang, M. Zhou, J. Cai, L. Liang, G. Ren, and L. Jiang, J. Mater. Chem. A **5**, 8070 (2017).
[49] H. W. Kim, M. B. Ross, N. Kornienko, L. Zhang, J. Guo, P. Yang, and B. D. McCloskey, Nat. Catal. **1**, 282 (2018).
[50] D. Tasis, N. Tagmatarchis, A. Bianco, and M. Prato, Chem. Rev. **106**, 1105 (2006).
[51] A. Khataee, M. Safarpour, M. Zarei, and S. Aber, J. Electroanal. Chem. **659**, 63 (2011).
[52] X. Zhang, J. Fu, Y. Zhang, and L. Lei, Sep. Purif. Technol. **64**, 116 (2008).
[53] S. Zhao, T. Guo, X. Li, T. Xu, B. Yang, and X. Zhao, Appl. Catal., B **224**, 725 (2018).
[54] K. Jiang, S. Back, A. J. Akey, C. Xia, Y. Hu, W. Liang, D. Schaak, E. Stavitski, J. K. Nørskov, and S. Siahrostami, Nat. Commun. **10**, 3997 (2019).
[55] C. H. Choi, H. C. Kwon, S. Yook, H. Shin, H. Kim, and M. Choi, J. Phys. Chem. C **118**, 30063 (2014).
[56] L.-Z. Peng, P. Liu, Q.-Q. Cheng, W.-J. Hu, Y. A. Liu, J.-S. Li, B. Jiang, X.-S. Jia, H. Yang, and K. Wen, Chem. Commun. **54**, 4433 (2018).
[57] Z. Zhao, M. Li, L. Zhang, L. Dai, and Z. Xia, Adv. Mater. **27**, 6834 (2015).
[58] Z. Zhao and Z. Xia, ACS Catal. **6**, 1553 (2016).
[59] C. W. Bezerra, L. Zhang, K. Lee, H. Liu, A. L. Marques, E. P. Marques, H. Wang, and J. Zhang, Electrochim. Acta **53**, 4937 (2008).
[60] N. Daems, X. Sheng, I. F. Vankelecom, and P. P. Pescarmona, J. Mater. Chem. A **2**, 4085 (2014).
[61] T. Asefa, Acc. Chem. Res. **49**, 1873 (2016).
[62] P. P. Olivera, E. M. Patrito, and H. Sellers, Surf. Sci. **313**, 25 (1994).
[63] M. Y. Oh, S. K. Park, H. Park, H. Kim, K. Kang, J. H. Kim, K. C. Roh, and T. H. Shin, ACS Appl. Energy Mater. **1**, 5518 (2018).
[64] S. Kim, D.-W. Lee, and K.-Y. Lee, J. Mol. Catal. A: Chem. **391**, 48 (2014).
[65] T. Deguchi and M. Iwamoto, J. Phys. Chem. C **117**, 18540 (2013).
[66] J. K. Edwards, B. Solsona, E. Ntainjua, A. F. Carley, A. A. Herzing, C. J. Kiely, and G. J. Hutchings, Science **323**, 1037 (2009).
[67] P. Landon, P. J. Collier, A. J. Papworth, C. J. Kiely, and G. J. Hutchings, Chem. Commun. **38**, 2058 (2002).
[68] M. Chen, D. Kumar, C.-W. Yi, and D. W. Goodman, Science **310**, 291 (2005).
[69] D. H. Wells, Jr., W. N. Delgass, and K. T. Thomson, J. Chem. Phys. **117**, 10597 (2002).
[70] R. Todorovic and R. Meyer, Catal. Today **160**, 242 (2011).
[71] M. Shao, J. Power Sources **196**, 2433 (2011).
[72] T. Pospelova, N. Kobozev, and E. Eremin, Russ. J. Phys. Chem. **35**, 143 (1961).
[73] Q. Liu, J. C. Bauer, R. E. Schaak, and J. H. Lunsford, Angew. Chem., Int. Ed. **47**, 6221 (2008).
[74] P. Landon, P. J. Collier, A. F. Carley, D. Chadwick, A. J. Papworth, A. Burrows, C. J. Kiely, and G. J. Hutchings, Phys. Chem. Chem. Phys. **5**, 1917 (2003).
[75] G. Li, J. Edwards, A. F. Carley, and G. J. Hutchings, Catal. Commun. **8**, 247 (2007).
[76] E. N. Ntainjua, S. J. Freakley, and G. J. Hutchings, Top. Catal. **55**, 718 (2012).
[77] B. E. Solsona, J. K. Edwards, P. Landon, A. F. Carley, A. Herzing, C. J. Kiely, and G. J. Hutchings, Chem. Mater. **18**, 2689 (2006).
[78] J. K. Edwards, B. Solsona, P. Landon, A. F. Carley, A. Herzing, M. Watanabe, C. J. Kiely, and G. J. Hutchings, J. Mater. Chem. **15**, 4595 (2005).
[79] J. Xu, L. Ouyang, G.-J. Da, Q.-Q. Song, X.-J. Yang, and Y.-F. Han, J. Catal. **285**, 74 (2012).
[80] R. Shen, W. Chen, Q. Peng, S. Lu, L. Zheng, X. Cao, Y. Wang, W. Zhu, J. Zhang, and Z. Zhuang, Chem **5**, 2099 (2019).
[81] J. K. Edwards, S. J. Freakley, A. F. Carley, C. J. Kiely, and G. J. Hutchings, Acc. Chem. Res. **47**, 845 (2014).
[82] J. Li and K. Yoshizawa, Catal. Today **248**, 142 (2015).
[83] D. W. Flaherty, ACS Catal. **8**, 1520 (2018).
[84] P. Rodriguez and M. T. Koper, Phys. Chem. Chem. Phys. **16**, 13583 (2014).
[85] J. Pritchard, L. Kesavan, M. Piccinini, Q. He, R. Tiruvalam, N. Dimitratos, J. A. Lopez-Sanchez, A. F. Carley, J. K. Edwards, and C. J. Kiely, Langmuir **26**, 16568 (2010).
[86] J. K. Edwards, B. E. Solsona, P. Landon, A. F. Carley, A. Herzing, C. J. Kiely, and G. J. Hutchings, J. Catal. **236**, 69 (2005).
[87] J. K. Edwards, J. Pritchard, M. Piccinini, G. Shaw, Q. He, A. F. Carley, C. J. Kiely, and G. J. Hutchings, J. Catal. **292**, 227 (2012).

[88]S. Kim, G.-H. Moon, H. Kim, Y. Mun, P. Zhang, J. Lee, and W. Choi, J. Catal. **357**, 51 (2018).
[89]J. Guan, D. Li, R. Si, S. Miao, F. Zhang, and C. Li, ACS Catal. **7**, 5983 (2017).
[90]H. Goto, Y. Hanada, T. Ohno, and M. Matsumura, J. Catal. **225**, 223 (2004).
[91]V. Viswanathan, H. A. Hansen, and J. K. Nørskov, J. Phys. Chem. Lett. **6**, 4224 (2015).
[92]K. Mase, M. Yoneda, Y. Yamada, and S. Fukuzumi, ACS Energy Lett. **1**, 913 (2016).
[93]R. Cai, Y. Kubota, and A. Fujishima, J. Catal. **219**, 214 (2003).
[94]K. Fuku, Y. Miyase, Y. Miseki, T. Gunji, and K. Sayama, ChemistrySelect **1**, 5721 (2016).
[95]M. Pelaez, N. T. Nolan, S. C. Pillai, M. K. Seery, P. Falaras, A. G. Kontos, P. S. Dunlop, J. W. Hamilton, J. A. Byrne, and K. O'shea, Appl. Catal., B **125**, 331 (2012).
[96]S. J. Moniz, S. A. Shevlin, D. J. Martin, Z.-X. Guo, and J. Tang, Energy Environ. Sci. **8**, 731 (2015).
[97]G. Kaur, O. Pandey, and K. Singh, Phys. Status Solidi A **209**, 1231 (2012).
[98]K. Fuku, Y. Miyase, Y. Miseki, T. Funaki, T. Gunji, and K. Sayama, Chem. - Asian J. **12**, 1111 (2017).
[99]K. Fuku, Y. Miyase, Y. Miseki, T. Gunji, and K. Sayama, RSC Adv. **7**, 47619 (2017).
[100]A. Nadar, S. S. Gupta, Y. Kar, S. Shetty, A. P. van Bavel, and D. Khushalani, J. Phys. Chem. C **124**, 4152 (2020).
[101]E. C. Paz, L. R. Aveiro, V. S. Pinheiro, F. M. Souza, V. B. Lima, F. L. Silva, P. Hammer, M. R. Lanza, and M. C. Santos, Appl. Catal., B **232**, 436 (2018).
[102]M. Campos, W. Siriwatcharapiboon, R. J. Potter, and S. L. Horswell, Catal. Today **202**, 135 (2013).
[103]V. S. Pinheiro, E. C. Paz, L. R. Aveiro, L. S. Parreira, F. M. Souza, P. H. Camargo, and M. C. Santos, Electrochim. Acta **259**, 865 (2018).
[104]J. F. Carneiro, M. J. Paulo, M. Siaj, A. C. Tavares, and M. R. Lanza, J. Catal. **332**, 51 (2015).
[105]J. F. Carneiro, R. S. Rocha, P. Hammer, R. Bertazzoli, and M. R. Lanza, Appl. Catal., A **517**, 161 (2016).
[106]A. Moraes, M. Assumpção, R. Papai, I. Gaubeur, R. S. Rocha, R. Reis, M. L. Calegaro, M. R. V. Lanza, and M. C. Santos, J. Electroanal. Chem. **719**, 127 (2014).
[107]T. Pengfei, L. Ouyang, X. Xinchao, X. Jing, and H. Yi-Fan, Chin. J. Catal. **34**, 1002 (2013).